Hierarchy of spin and valley symmetry breaking in quantum Hall single-layer graphene

Zhihua Yang and Jung Hoon Han*
Department of Physics, Sungkyunkwan University, Suwon 440-746, Korea
(Received 16 October 2009; revised manuscript received 28 December 2009; published 3 March 2010)

Several microscopic mechanisms for breaking the fourfold degeneracy of the central Landau level in a single-layer graphene is examined. We consider valley-scattering random potential, Zeeman interaction, and electron-phonon coupling as potential candidates to break the SU(4) symmetry of the Coulomb exchange interaction. A phase diagram is worked out, giving either the "spin-first" or "valley-first" splitting of the central Landau levels depending on the relative strengths of the electron-phonon coupling and the Zeeman interaction. Existence of a midgap band at the domain wall separating Landau levels of opposite valley polarity is demonstrated.

DOI: 10.1103/PhysRevB.81.115405 PACS number(s): 73.43.Cd, 73.50.−h, 73.61.Wp

I. INTRODUCTION

Spin and valley degeneracies of a single-layer graphene sheet subject to a perpendicular magnetic field gives rise to a quantized Hall conductance[1,2] σ_{xy} that changes in multiples of four units of conductance quantum e^2/h. Taking $e^2/h \equiv 1$, the conductance changes from −2 to +2 directly as the chemical potential passes through the central Landau level (LL). When the strength of the magnetic field increases, these fourfold-degenerate LL's split in energy into two sublevels,[3–5] and accordingly the Hall conductance steps occur at −2, 0, and +2. At even higher fields, the fourfold degeneracy is broken completely, leading to the sequence $-2,-1,0,1,2$.[3–5]

The mechanics of the breaking of fourfold degeneracy of the central LL in graphene has been discussed in a large number of papers.[6–23] The SU(4) symmetry of the pristine central LL can be broken spontaneously from interaction effects or due to a number of possible weak symmetry-breaking interactions. Among the effects, the exchange part of the Coulomb interaction can lead to the spontaneous breaking of either spin or valley symmetry, or some mixture thereof.[6–8,24,25] The Zeeman effect breaks SU(2)-spin symmetry explicitly, and favor the spin symmetry breaking of the central LL over the valley symmetry breaking. On the other hand, magnetic field induced in-plane and out-of-plane lattice distortions[9–11] provide the mechanism to lift the valley degeneracy. The out-of-plane displacement of *a*-sublattice atoms opposite in direction to that of *b*-sublattice sites results in the charge-density-wave (CDW) state. The in-plane distortion of the carbon-carbon bonds as mediated by the optical *K* phonon gives rise to dimerized bond patterns (Kekulé distortion). The CDW order represents the valley spin ordering along the *z* direction of the pseudospin space while the Kekulé order represents the XY ordering of the pseudospin. A possible list of SU(4) symmetry-breaking terms are nicely summarized in a recent paper by Nomura *et al.*[11] The charge-carrying midgap states arising from defects in the Kekulé pattern has been analyzed in detail by Hou *et al.*[10] The discussions in Nomura *et al.*'s paper and of Hou *et al.* rely in an essential manner on the existence of the XY-ordered valley gap. The origin of the valley order itself, however, was not carefully addressed in either of the papers and our work complements these prior works by trying to identify the origin of valley order in greater detail. Influence of random on site and bond disorder[12–14] as well as the strain-induced random magnetic field[15] on symmetry breaking were also studied.

The focus of recent discussion has been whether the hierarchy of symmetry breaking upon increasing the magnetic field strength would be "spin-first, valley-later" or the opposite. Abanin *et al.* first pointed out that if the spin symmetry was broken but not the valley symmetry, the edge of the Hall sample will remain conducting due to counterpropagating edge channels.[16] No such conducting edge channels are guaranteed if the valley splitting occurred in the bulk of the Hall bar. An experiment carried out shortly thereafter seems to confirm the existence of conducting channels associated with the edge of the central LL.[4] On the other hand, subsequent transport experiments[26] which found divergent longitudinal resistance seem to rule out the existence of such gapless edge states, and the issue of "spin-first" or "valley-first" symmetry breaking appears by no means settled.

As the main SU(4)-invariant Coulomb interaction has no way to favor one degeneracy lifting over the other, which one of the spin and valley symmetries is lifted first depends sensitively on the relative strengths of residual interactions that do not preserve SU(4) invariance. In other words, it is the competition between those residual interactions that define the hierarchy problem of symmetry breaking in the central LL. In this paper, we address this issue within the self-consistent Hartree-Fock (HF) theory at half filling (two out of four central LL's filled) and quarter filling (one LL filled) while including several SU(4) symmetry-breaking terms explicitly within the same HF scheme. Although these symmetry-breaking terms were analyzed individually or in combination by many authors in the past, it is our belief that none has addressed the problem as a "competition" between different symmetry-breaking tendencies or used the self-consistent HF scheme to treat all interaction effects on an equal footing.

The paper is organized as follows. In Sec. II, we introduce several microscopic symmetry-breaking mechanisms in addition to the Coulomb interaction-Zeeman effect, valley-scattering impurity, and electron-phonon interaction-all of which have the potential to break spin or valley degeneracy. In Sec. III, we discuss the phase diagram that results mainly

from the competition between Zeeman field and electron-phonon interaction. In Sec. IV, we demonstrate the existence of midgap energy bands between Landau levels of opposite valley polarity and consider the edge behavior for valley-polarized states. A summary is given in Sec. V.

II. HARTREE-FOCK THEORY

Following the standard approach, we adopt the continuum description of the graphene dynamics using the spinor $\psi_{\sigma\tau}(r)=\left[\begin{smallmatrix}a_{\sigma\tau}(r)\\ b_{\sigma\tau}(r)\end{smallmatrix}\right]$. Spin ($\sigma=\uparrow,\downarrow$) and valley index $\tau=\pm$ are introduced to classify the spinors formed from a- and b-sublattice electrons. The Landau level problem with the perpendicular magnetic field can be treated by the Hamiltonian,

$$H^{\mathrm{K}}=\hbar\omega i\sum_{\sigma\tau}\int_r \psi^{\dagger}_{\sigma\tau}(r)\begin{pmatrix}0 & -\mathcal{A}\\ \mathcal{A}^{+} & 0\end{pmatrix}\psi_{\sigma\tau}(r), \tag{1}$$

where $\int_r$ means $\int d^2r$. With the noncommuting operators obeying $[p_x,p_y]=i\hbar^2/l_B^2$, one can form a set of canonical operators $\mathcal{A}=(l_B/\sqrt{2}\hbar)(p_x+ip_y)$, $\mathcal{A}^{+}=(l_B/\sqrt{2}\hbar)(p_x-ip_y)$, $[\mathcal{A},\mathcal{A}^{+}]=1$. A Fermi velocity v_F, magnetic length $l_B=\sqrt{\hbar/eB}$, and the cyclotron frequency $\omega=\sqrt{2}v_F/l_B$ have been introduced. We have implemented the rotation of the $\tau=-$ spinor, $\psi_{\sigma-}\rightarrow\sigma_y\psi_{\sigma-}$, in arriving at the Hamiltonian in the manifestly SU(4) symmetric form above. Using the complete set of normalized eigenfunctions given by

$$\chi_{nm}=\frac{1}{\sqrt{2}}\begin{pmatrix}\mathrm{sgn}(n)\phi_{|n|-1,m}\\ i\phi_{|n|m}\end{pmatrix},\quad \chi_{0m}=\begin{pmatrix}0\\ \phi_{0m}\end{pmatrix}, \tag{2}$$

one may expand the field operator as

$$\psi_{\sigma\tau}(r)=\sum_{n,m}\chi_{nm\tau}(r)\gamma_{nm\sigma\tau}, \tag{3}$$

where $\gamma_{nm\sigma\tau}$ is the eigenoperator of a given LL index n, guiding center coordinate m, and spin and valley indices σ and τ. Here ϕ_{nm} is the oscillator wave function and $\chi_{nm\tau}$ equals χ_{nm} defined in Eq. (2) if $\tau=+$ but equals $\sigma_y\chi_{nm}$ when $\tau=-$.

As the primary interest of this paper is in understanding the mechanism of level splitting within the central LL, we carry out the projection to $n=0$ LL states. Physically, the LL separation is also the largest energy scale of the problem. The kinetic energy gets completely quenched whereas Coulomb interaction within this LL would read

$$H^{\mathrm{C}}=\frac{1}{2}\int_{r,r'}V(r-r')\sum_{\substack{m_1,m_2,m_3,m_4\\ \sigma,\sigma',\tau,\tau'}}\phi^{*}_{m_4}(r)\phi_{m_1}(r)\phi^{*}_{m_3}(r')\phi_{m_2}(r')\gamma^{\dagger}_{m_4\sigma\tau}\gamma^{\dagger}_{m_3\sigma'\tau'}\gamma_{m_2\sigma'\tau'}\gamma_{m_1\sigma\tau}. \tag{4}$$

The reference to the LL index $n=0$ has been dropped. For numerical purpose, we assume a torus geometry of dimension $L_x\times L_y$ and use the Landau gauge for which the wave functions are

$$\phi_m(r)=\frac{1}{\pi^{1/4}L_x^{1/2}}e^{ik_mx}e^{-1/2(y-k_m)^2},\quad k_m=\frac{2\pi}{L_x}m. \tag{5}$$

The Coulomb Hamiltonian in this basis reads

$$H^{\mathrm{C}}=\frac{1}{2L_xL_y}\sum_{\substack{m_x,m_y\\ m_1,m_2}}V(k_x,k_y)e^{-k_x^2/2-k_y^2/2+ik_y(k_{m_1}-k_{m_2}+k_x)}\sum_{\sigma\sigma'\tau\tau'}\gamma^{\dagger}_{m_1+m_x\sigma\tau}\gamma^{\dagger}_{m_2-m_x\sigma'\tau'}\gamma_{m_2\sigma'\tau'}\gamma_{m_1\sigma\tau}, \tag{6}$$

where the Fourier-transformed Coulomb potential $V(k)=\int_r V(r)e^{ikr}$ is shown. The two momentum coordinates k_x and k_y are discretized, $k_x=2\pi m_x/L_x$ and $k_y=2\pi m_y/L_y$, where m_x and m_y will run over all integers. The guiding center coordinates m_1 and m_2 span 1 through N_ϕ, the number of flux through the lattice N_ϕ being given by $2\pi N_\phi=L_xL_y$.

Having established a discretized Coulomb Hamiltonian, we solve it within the Hartree-Fock theory using the self-consistent parameter,

$$\Delta_{\sigma_1\tau_1,\sigma_2\tau_2}(m_1,m_2)=\langle\gamma^{\dagger}_{m_1\sigma_1\tau_1}\gamma_{m_2\sigma_2\tau_2}\rangle \tag{7}$$

with an arbitrary pair of guiding center indices m_1,m_2 and the spin-valley indices. For the reason that Hartree term offers only a chemical-potential shift in the case of uniform solutions, and that it does not break the SU(4) symmetry, we will from now on exclusively concentrate on the exchange part of the Coulomb Hamiltonian, H^{EX}.

Among the possible SU(4) symmetry-breaking terms, we consider the following three:

(1) Zeeman field H^{B}: $H^{\mathrm{B}}=B_\sigma\Sigma_{m\sigma\tau}\sigma\gamma^{\dagger}_{m\sigma\tau}\gamma_{m\sigma\tau}$, where $B_\sigma=g\mu_BB/2$, μ_B is the Bohr magneton and the Lande factor in graphene $g\simeq 2$.

(2) Valley-scattering impurity H^{imp},

$$H^{\text{imp}} = \sum_{m\sigma\tau} V_m \gamma^{\dagger}_{m\sigma\tau}\gamma_{m\sigma\bar{\tau}}, \tag{8}$$

where $\bar{\tau}=-\tau$. We take V_m as a random number of width W: $V_m \in [-W/2, W/2]$.

(3) Valley-scattering electron-phonon coupling,[11]

$$H^{\text{el-ph}} = -\sqrt{2\pi}U \int_r \sum_{\sigma\sigma'\tau} (\psi^{\dagger}_{\sigma\tau}\sigma_x\psi_{\sigma\bar{\tau}})(\psi^{\dagger}_{\sigma'\bar{\tau}}\sigma_x\psi_{\sigma'\tau}). \tag{9}$$

Projected onto the central LL and treated in the mean-field manner, this last Hamiltonian becomes

$$H^{\text{el-ph}}_{\text{MF}} = -U\sum_{m\sigma\tau}\left[\sum_{\sigma'}\Delta_{\sigma'\tau,\sigma'\bar{\tau}}(m,m)\right]\gamma^{\dagger}_{m\sigma\bar{\tau}}\gamma_{m\sigma\tau}. \tag{10}$$

Note that only those elements of the mean-field order with the same guiding center coordinates are considered in reaching Eq. (10). As it turns out, a completely general HF calculation allowing a nonlocal order parameter $\Delta_{\sigma_1\tau_1,\sigma_2\tau_2}(m_1,m_2)$, $m_1\neq m_2$ yields values which are almost an order of magnitude smaller when $|m_1-m_2|=1$ than if $m_1=m_2$. Further increase in $|m_1-m_2|$ yields even smaller order parameters. Then, to an excellent approximation, we can regard the HF order parameters as local in the guiding center index m. Motivated by this observation, we have also neglected the $m_1\neq m_2$ contribution in writing down the impurity Hamiltonian, Eq. (8). Therefore the Hartree-Fock Hamiltonian we consider is of the block form, $H=\Sigma_m H_m$ with each H_m given as the sum $H_m=H^{\text{EX}}_m+H^B_m+H^{\text{imp}}_m+H^{\text{el-ph}}_m$ and each piece of the Hamiltonian given by

$$H^{\text{EX}}_m = -\frac{1}{2\pi N_\phi}\sum_{\substack{\sigma_1,\tau_1,\\ \sigma_2,\tau_2}}\gamma^{\dagger}_{m\sigma_2\tau_2}\left[\sum_{m_x,m_y=-\infty}^{\infty} V\left(\frac{2\pi m_x}{L_x},\frac{2\pi m_y}{L_y}\right)\right.$$
$$\times e^{-1/2(2\pi m_x/L_x)^2-1/2(2\pi m_y/L_y)^2}$$
$$\left.\times\Delta_{\sigma_1\tau_1,\sigma_2\tau_2}(m+m_x,m+m_x)\right]\gamma_{m\sigma_1\tau_1},$$

$$H^B_m = B_\sigma\sum_{\sigma\tau}\sigma\gamma^{\dagger}_{m\sigma\tau}\gamma_{m\sigma\tau},$$

$$H^{\text{imp}}_m = V_m\sum_{\sigma\tau}\gamma^{\dagger}_{m\sigma\tau}\gamma_{m\sigma\bar{\tau}},$$

$$H^{\text{el-ph}}_m = -U\sum_{\sigma\tau}\left[\sum_{\sigma'}\Delta_{\sigma'\tau,\sigma'\bar{\tau}}(m,m)\right]\gamma^{\dagger}_{m\sigma\bar{\tau}}\gamma_{m\sigma\tau}. \tag{11}$$

Although it may seem that different m's are disconnected, in fact they are related to one another through the self-consistency relationship. At this point, it should be clear that the main competitive tendency in our model arises from the spin polarization inherent in H^B_m and the valley polarization implied by H^{imp}_m and $H^{\text{el-ph}}_m$.

We made extensive numerical simulation at zero temperature of the full mean-field Hamiltonian, as well as the simplified one given in Eq. (11), to carve out the mechanism of symmetry breaking due to the Zeeman, valley-scattering impurity, and electron-phonon coupling-induced interactions. Both quarter-filled (one out of four LLs occupied) and half-filled (two out of four central LLs occupied) cases were examined. The 3/4-filled case can be deduced by symmetry from the results of 1/4-filled case.

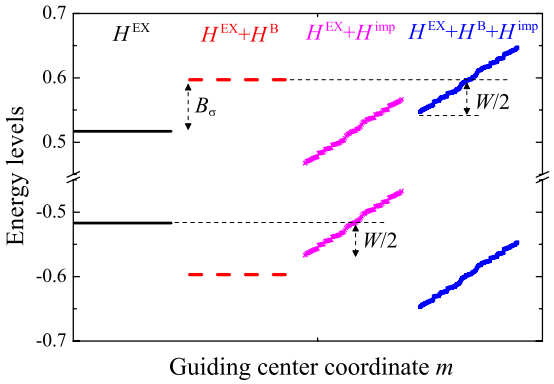

FIG. 1. (Color online) Plot of the energy levels at half filling obtained from self-consistent HF calculation. The x axis represents the guiding center coordinate m which takes values from 1 to N_ϕ. The Hamiltonian under consideration is (from left to right) H^{EX} (black solid lines), $H^{\text{EX}}+H^{\text{B}}$ (red dash lines), $H^{\text{EX}}+H^{\text{imp}}$ (magenta crosses), and $H^{\text{EX}}+H^{\text{B}}+H^{\text{imp}}$ (blue filled squares). The impurity broadening is $W=0.1$ and the Zeeman field is $B_\sigma=0.08$. The system size used is $N_\phi=50$.

III. PHASE DIAGRAM OF THE CENTRAL LANDAU LEVEL

With H^{EX} alone and at half filling, the initial fourfold degeneracy of the LL is split into two sublevels with energies at $\pm E^{\text{EX}}$, where the energy scale E^{EX} is set by the exchange energy interaction. In our convention, $e^2/\kappa l_B$ (κ=dielectric constant) is taken to unity, and in such a unit, we obtain $E^{\text{EX}}\approx 0.52$. For the quarter-filled case, a similar situation arises with one LL at an energy below the chemical potential and three degenerate LL's whose energy lies above it. One can learn from these exercises that the full energy splitting of the central LL requires more than the Coulomb exchange effect alone. At this point, which of the spin and valley symmetries remains intact is completely arbitrary.

Inclusion of the Zeeman field to the Coulomb exchange now ensures that the symmetry breaking occurs along the spin direction, with the LL energies at $\pm(E^{\text{EX}}+B_\sigma)$ for half filling and the chemical potential equal to zero. The valley-SU(2) symmetry is preserved under the addition of H^B. In order to break the remaining valley symmetry, an additional symmetry-breaking term acting along the valley direction is called for. The intervalley impurity scattering term H^{imp} does break the valley symmetry somewhat, as the previously twofold-degenerate states for each guiding center m undergoes splitting by $\pm V_m$. On average, as shown in Fig. 1, the overall level broadening due to the impurity scattering does not result in the clear splitting of the valley degeneracy.

In searching for a physically transparent mechanism of valley symmetry breaking, we first analyze the following toy model consisting of the Coulomb exchange Hamiltonian per-

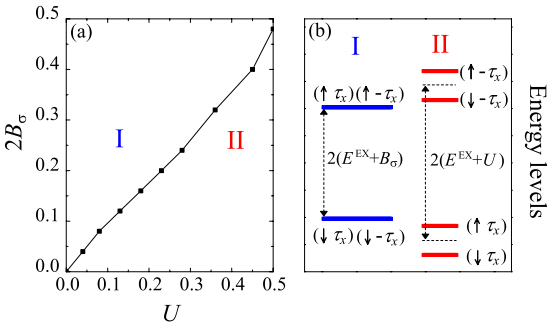

FIG. 2. (Color online) (a) Phase diagram of the central LL at half filling with varying Zeeman field ($2B_\sigma$) and electron-phonon coupling strength (U). In region I ($2B_\sigma \gtrsim U$), only the spin degeneracy is broken while the valley symmetry remains preserved. In region II ($U \gtrsim 2B_\sigma$), both spin and valley symmetries are lost but the main level splitting takes place in the valley direction. A first-order phase boundary separates the two regions. (b) Schematic LL energy levels in each region, where the index $\pm\tau_x$ refers to the two valley eigenstates polarized along the x direction. The energy-level separations and spin-valley quantum numbers for each LL are specified.

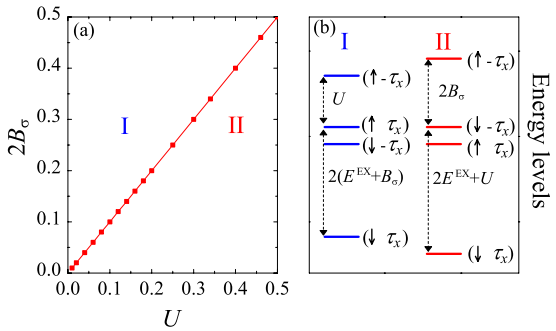

FIG. 3. (Color online) Phase diagram of the central LL at quarter filling. Meaning of the symbols are the same as in Fig. 2. Only one LL lies below the Fermi level here.

turbed by two kinds of Zeeman fields separately acting on the spin and valley spaces:

$$H^{EX} + B_\sigma \sum_{m\sigma\tau} \sigma \gamma^+_{m\sigma\tau}\gamma_{m\sigma\tau} + B_\tau \sum_{m\sigma\tau} \gamma^+_{m\sigma\bar{\tau}}\gamma_{m\sigma\tau}. \quad (12)$$

In keeping with the discussion on the electron-phonon coupling mechanism that will follow, we applied the valley Zeeman field in the x direction. An SU(2) rotation in the valley space can orient the valley Zeeman field along the z axis without altering other parts of the Hamiltonian. This model does exhibit a full lifting of the fourfold degeneracy with the LL energies given at $(E^{EX}+B_M)\pm B_m$ and at $-(E^{EX}+B_M)\pm B_m$, where B_M and B_m refer to the larger and the smaller of the two Zeeman fields, respectively. Actually, the electron-phonon coupling Hamiltonian $H^{el\text{-}ph}_{MF}$ provides the required valley Zeeman field, acting along the x axis of the valley spin with the field strength $B_\tau \sim U\Sigma_\sigma \Delta_{\sigma-,\sigma+}(m,m)$. The relevant valley eigenstates here would be those given by $|\tau_x=+\rangle = (|\tau_z=+\rangle + |\tau_z=-\rangle)/\sqrt{2}$ and $|\tau_x=-\rangle = (|\tau_z=+\rangle - |\tau_z=-\rangle)/\sqrt{2}$.

Aided by these ideas, we considered the level-splitting scheme implied in $H^{EX}+H^B+H^{el\text{-}ph}_{MF}$. Figure 2 shows the phase diagram for such a model, at half filling, spanned by two interaction parameters $(U, 2B_\sigma)$. There are two phases found here, called I and II, distinguished by their main polarization directions. In region I, where the Zeeman effect dominates, only one, spin-polarized level splitting is observed. The valley-splitting order parameter $\Delta_{\sigma-,\sigma+}(m,m)$ is self-consistently reduced to zero in this region, thereby preserving the valley symmetry. In the U-dominated region II, the main splitting is that of valley degeneracy while the Zeeman field contributes to the sublevel splitting equal to $2B_\sigma$. The phase boundary taking place along $2B_\sigma \approx U$ in the phase diagram is first order.

The phase diagram for quarter filling is similar as shown in Fig. 3. The phase boundary now taking place exactly at $2B_\sigma = U$ separates the spin-first-split region I from the valley-first-split region II. The two inner LL's cross in energy at the phase boundary. For instance, $E(\uparrow, \tau_x=+) > E(\downarrow, \tau_x=-)$ energy hierarchy in region I crosses over to $E(\uparrow, \tau_x=+) < E(\downarrow, \tau_x=-)$ in region II. We have checked that the inclusion of the impurity does not alter the basic features of the phase diagrams shown in Figs. 2 and 3 as long as W remains small compared to both U and $2B_\sigma$. For W exceeding both Zeeman and electron-phonon energy scales, a rather different picture of the hierarchical level splitting might result.[12–14] The weak-impurity picture proposed in this paper will hold better for the suspended graphene samples, which are nearly free of the short-range impurities.[27]

The relevant energy scales $2B_\sigma$ and U in a single-layer graphene are estimated at $2B_\sigma \sim 1.3B$ [K/T] (Ref. 5) and $U \sim 2/\sqrt{2\pi B}$ [K/T] $\sim 0.8B$ [K/T].[11,28] Given the proximity of the two energy scales and the crudeness of the estimates involved, however, we feel that it is more reasonable to regard some graphene samples to be characterized by $2B_\sigma > U$ while others fall into the parameter range $2B_\sigma < U$.

Take a sample with $2B_\sigma > U$ (region I of Figs. 2 and 3) and imagine varying the chemical potential through $1/4 \to 1/2 \to 3/4$ filling of the central LL. The occupied LL's are given by $(\downarrow, \tau_x)$ at 1/4 filling, successively enclosing $(\downarrow, \bar{\tau}_x)$ and $(\uparrow, \tau_x)$ LL's at 1/2 and 3/4 filling, respectively. For a sample in region II, the sequence of filled LL's reads $(\downarrow, \tau_x)$, $(\uparrow, \tau_x)$, and $(\downarrow, \bar{\tau}_x)$. Therefore, when the spin-polarization tendency is stronger (region I), the valley quantum numbers are quenched at half filling. If the valley polarization tendency dominates (region II), a spin-quenched state at half filling is obtained instead. It follows that with either I or II, sweeping the chemical potential should allow one to see "one Landau level at a time" and lead to Hall conductance steps increasing in one e^2/h unit. What limits this resolution is presumably extrinsic effects such as the amount of impurity level broadening exceeding the Zeeman and/or the electron-phonon coupling energies. Even in the pure case, however, the transverse conductance measurement alone proves to be an inadequate probe of the hierarchical structure of the central LL splitting. In the next section, we develop the idea of probing the bulk quantum numbers through the examination of the edge behavior.[16,22]

Before closing this section, we remark that a transition between the spin-dominant and valley-dominant regions dis-

TABLE I. Summary of the main polarization direction, nature of the half-filled ground state, and the edge behavior for spin-dominant (region I) and valley-dominant (region II) graphene samples at central LL.

Region	Primary polarization	At half filling	Edge behavior
$2B_\sigma > U$	Spin	Valley quenched	Conducting
$U > 2B_\sigma$	Valley	Spin quenched	Insulating

cussed in this section might be achieved through the control of the electron-phonon coupling strength U. We speculate that applying a mechanical pressure through stretching to the graphene will be able to influence U without changing the Zeeman energy. Several papers examined the influence of mechanical stretching on the electronic band structure recently.[29] It is hoped that an extension of those analysis will tell us if the phonon spectrum and the strength of electron-phonon coupling can also be significantly modified by the stretching. The bond-CDW order associated with region II at half filling and regions I and II for quarter filling should leave a mark in the electronic spectrum, which can be probed by STM.

IV. DOMAIN BOUNDARIES AND EDGES

We begin this section with a simple observation: a Landau level with a quantum number (σ, τ_x) occurs at the same energy as another state with $(\sigma, \bar{\tau}_x)$ whereas the same is not true with $(\bar{\sigma}, \tau_x)$ due to the Zeeman splitting of the two spin states. We therefore expect that domain walls separating the two macroscopically distinct valley states should occur quite naturally. Physically, the two macroscopic states correspond to two possible Kekulé distortions of the graphene lattice, and the domain wall would be a one-dimensional string of broken bonds.

Take region I at half filling which, according to Fig. 2 and Table I, is valley quenched. In this case, no domain-wall structure of the valley index is expected. On the other hand, region II at half filling is spin quenched, with its valley quantum number taking either $\tau_x=+1$ or $\tau_x=-1$. A domain wall separating the two distinct Kekulé patterns can be formed. A quarter-filled LL always allows a valley domain wall as it is occupied by only one of the valley states.

The physics of the valley domain wall can be captured in a set of differential equations,

$$
\begin{aligned}
i(\partial_y + y_k)[u_- + v_+] + m_v(y)[u_+ - v_-] &= -\varepsilon_k[u_+ - v_-],\\
i(\partial_y - y_k)[u_+ - v_-] - m_v(y)[u_- + v_+] &= -\varepsilon_k[u_- + v_+],\\
i(\partial_y + y_k)[u_- - v_+] + m_v(y)[u_+ + v_-] &= \varepsilon_k[u_+ + v_-],\\
i(\partial_y - y_k)[u_+ + v_-] - m_v(y)[u_- - v_+] &= \varepsilon_k[u_- - v_+], \quad (13)
\end{aligned}
$$

where the spinless case was assumed for simplicity. We have written the eigenfunction associated with the a- and b-sublattice sites as (u_τ, v_τ), which are also distinguished by their valley index τ, used the linear gauge $(A_x=-By,\ A_y=0)$, and taken out the x dependence of the wave function by writing $(u_\tau, v_\tau) \to e^{ikx}[u_\tau(y), v_\tau(y)]$. The y-dependent mass gap due to the valley mixing is written as $m_v(y)$ and y_k abbreviates $y-k$. In accordance with the Hartree-Fock calculation of the previous section, we assumed that the mixing occurs along the x direction in valley space.

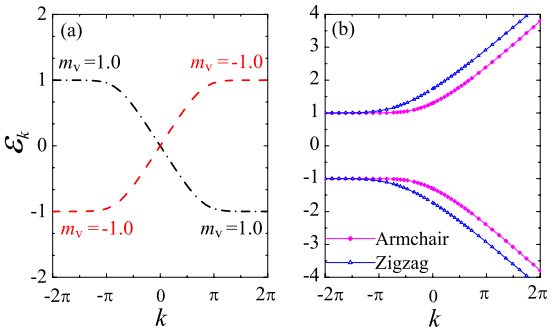

FIG. 4. (Color online) (a) The energy ε_k obtained from Eq. (14) with $m_v=1.0$ and (b) the energy spectra in the cases of armchair and zigzag boundaries with $m_v=1.0$.

For illustration of the influence of the valley domain wall on the energy spectra, consider the case with an abrupt sign change in the mass gap: $m_v(y)=m_v\ \mathrm{sgn}(y)$. Well away from $y=0$, the mass gap is uniform and a pair of solutions with $\varepsilon_k=\pm m_v$ is found for $u_+=v_-=0$ and $u_-=\pm v_+=\phi(y-k)$, respectively, where $\phi(y-k)$ is the Gaussian function peaked at $y=k$. Since k is still a good quantum number in the presence of the y-dependent mass $m_v(y)$, the eigen energies ε_k can be solved for each k separately. By matching the wave functions at $y=0$, we derive the following equation determining the energies:

$$
\frac{m_v - \varepsilon_k}{m_v + \varepsilon_k} = \frac{H(p_k,k)H'(p_k,-k)}{H(p_k,-k)H'(p_k,k)} = \frac{H(p_k,k)H(p_k-1,-k)}{H(p_k,-k)H(p_k-1,k)},
$$

$$
p_k = (\varepsilon_k^2 - m_v^2)/2. \quad (14)
$$

Here $H(p_k,k)$ is a Hermite function of order p_k, and we used the identity $\partial_y H(p_k,y_k)=2p_k H(p_k-1,y_k)$ in reaching the last expression in Eq. (14). Self-consistently solving the equation for each k gives rise to a pair of midgap bands shown in Fig. 4(a).

The level crossing predicted here is of particular relevance when the chemical potential lies between the two valley-split LL's. In such a case, a pair of gapless one-dimensional channels will cross the Fermi level, similar to the edge channel in the spin-split case first discussed in Ref. 16. Unlike the edge channels, the metallic channel predicted here can be formed at the bulk whenever a domain boundary separates the opposite valley states.

It had been argued previously that a pair of valley-split central LL states with $\tau_z=\pm 1$ will not result in metallic edge channels at half filling.[16,22] In our case, the valley splitting is along the x direction, which therefore mixes the $\tau_z=\pm 1$ states, and some question might arise as to whether the edge nature will be any different from the $\tau_z=\pm 1$ bulk case discussed previously. The answer is provided by analyzing the same set of equations, Eq. (13), with either armchair or zig-

zag boundary conditions imposed on the wave functions. Taking the physical graphene space to be $y<0$, we arrive at the following equations for the two boundary conditions:

$$\frac{[H(p_k,k)]^2}{[H(p_k-1,k)]^2}=2p_k, \quad \text{(armchair)},$$

$$H(p_k-1,k)=0, \quad \text{(zigzag)}. \tag{15}$$

As shown in Fig. 4(b), we do not find gapless channels in either boundary conditions, consistent with prior claims for $\tau_z\pm 1$ valley-split case.[16] The metallicity of the edge is hence a good indicator of the spin- or valley-quenched character of the half-filled central LL. The findings of our investigation are summarized in Table I.

V. SUMMARY

In summary, we examined the spin-first or valley-first, or the hierarchy issue of the central LL symmetry breaking of a graphene layer. Using the method of self-consistent Hartree-Fock theory, several kinds of SU(4) symmetry-breaking terms were considered simultaneously, together with the Coulomb exchange Hamiltonian. A particular attention was given to the competitive nature of the valley-splitting (due to electron-phonon interaction) and spin-splitting (due to Zeeman interaction) tendencies.

We obtain a phase diagram which exhibits either a spin-first or a valley-first level splitting depending on the relative dominance of the Zeeman energy B_σ and the electron-phonon coupling energy U. We conclude that the Hall conductance steps upon varying the filling factor should, in principle, reveal all Landau sublevels in either regimes, as long as the amount of impurity broadening is weak enough. The half-filled central LL is either valley quenched (region I, $2B_\sigma>U$) or spin quenched (region II, $U>2B_\sigma$), reflecting the tendency to quench the weaker of the two order parameters first.

Finally, the energy level structure near the sample boundary or at the domain wall separating the opposite valley states were examined. The mass gap present in the Kekulé-ordered graphene lattice is shown to have the insulating edge behavior. By contrast, a domain wall separating the two types of Kekulé-distorted lattices is shown to support a pair of midgap bands, with the potential for forming a one-dimensional metallic channel in the bulk of the graphene sample.

ACKNOWLEDGMENTS

H. J. H. is supported by the Korea Science and Engineering Foundation (KOSEF) grant funded by the Korea government (MEST) (Grant No. R01-2008-000-20586-0), and in part by the Asia Pacific Center for Theoretical Physics. One of us (H. J. H.) wishes to thank P. Kim for hospitality during the completion of this work and for a discussion that prompted this project.

*hanjh@skku.edu

[1] K. S. Novoselov, A. K. Geim, S. V. Morozov, D. Jiang, M. I. Katsnelson, I. V. Grigorieva, S. V. Dubonos, and A. A. Firsov, Nature (London) **438**, 197 (2005).
[2] Y. Zhang, Y.-W. Tan, H. L. Stormer, and P. Kim, Nature (London) **438**, 201 (2005).
[3] Y. Zhang, Z. Jiang, J. P. Small, M. S. Purewal, Y.-W. Tan, M. Fazlollahi, J. D. Chudow, J. A. Jaszczak, H. L. Stormer, and P. Kim, Phys. Rev. Lett. **96**, 136806 (2006).
[4] D. A. Abanin, K. S. Novoselov, U. Zeitler, P. A. Lee, A. K. Geim, and L. S. Levitov, Phys. Rev. Lett. **98**, 196806 (2007).
[5] Z. Jiang, Y. Zhang, H. L. Stormer, and P. Kim, Phys. Rev. Lett. **99**, 106802 (2007).
[6] K. Nomura and A. H. MacDonald, Phys. Rev. Lett. **96**, 256602 (2006).
[7] M. O. Goerbig, R. Moessner, and B. Douçot, Phys. Rev. B **74**, 161407(R) (2006).
[8] J. Alicea and M. P. A. Fisher, Phys. Rev. B **74**, 075422 (2006).
[9] J. N. Fuchs and P. Lederer, Phys. Rev. Lett. **98**, 016803 (2007).
[10] C.-Y. Hou, C. Chamon, and C. Mudry, Phys. Rev. Lett. **98**, 186809 (2007); Phys. Rev. B **81**, 075427 (2010).
[11] K. Nomura, S. Ryu, and D.-H. Lee, Phys. Rev. Lett. **103**, 216801 (2009).
[12] D. N. Sheng, L. Sheng, and Z. Y. Weng, Phys. Rev. B **73**, 233406 (2006).
[13] L. Sheng, D. N. Sheng, F. D. M. Haldane, and L. Balents, Phys. Rev. Lett. **99**, 196802 (2007).
[14] M. Koshino and T. Ando, Phys. Rev. B **75**, 033412 (2007).
[15] D. A. Abanin, P. A. Lee, and L. S. Levitov, Phys. Rev. Lett. **98**, 156801 (2007).
[16] D. A. Abanin, P. A. Lee, and L. S. Levitov, Phys. Rev. Lett. **96**, 176803 (2006).
[17] K. Yang, S. Das Sarma, and A. H. MacDonald, Phys. Rev. B **74**, 075423 (2006).
[18] K. Yang, Solid State Commun. **143**, 27 (2007).
[19] I. F. Herbut, Phys. Rev. B **75**, 165411 (2007).
[20] M. Ezawa, J. Phys. Soc. Jpn. **76**, 094701 (2007).
[21] V. P. Gusynin, V. A. Miransky, S. G. Sharapov, and I. A. Shovkovy, Phys. Rev. B **74**, 195429 (2006).
[22] V. P. Gusynin, V. A. Miransky, S. G. Sharapov, and I. A. Shovkovy, Phys. Rev. B **77**, 205409 (2008).
[23] B. Douçot, M. O. Goerbig, P. Lederer, and R. Moessner, Phys. Rev. B **78**, 195327 (2008).
[24] D. P. Arovas, A. Karlhede, and D. Lilliehook, Phys. Rev. B **59**, 13147 (1999).
[25] D. V. Khveshchenko, Phys. Rev. Lett. **87**, 206401 (2001).
[26] J. G. Checkelsky, L. Li, and N. P. Ong, Phys. Rev. Lett. **100**, 206801 (2008); Phys. Rev. B **79**, 115434 (2009).
[27] K. I. Bolotin, K. J. Sikes, J. Hone, H. L. Stormer, and P. Kim, Phys. Rev. Lett. **101**, 096802 (2008).
[28] N. A. Viet, H. Ajiki, and T. Ando, J. Phys. Soc. Jpn. **63**, 3036 (1994); H. Ajiki and T. Ando, *ibid.* **64**, 260 (1995); **65**, 2976 (1996).
[29] S. Choi, S. Jhi, and Y. Son, Phys. Rev. B **81**, 081407(R) (2010), and references therein.